



## Abstract

Using the SDSS-V Local Volume Mapper (LVM), an optical integral field spectrograph, we spatially map the physical conditions of the Trifid Nebula (M 20) at approximately 0.24 pc resolution. The different emission lines measured with LVM (e.g. Hydrogen recombination lines and collisional excited lines: [OII] $\lambda\lambda$ 3727,29; [SII] $\lambda$ 4069; [OIII] $\lambda$ 5007; [NII] $\lambda$ 5755; [SIII] $\lambda$ 6312; [NII] $\lambda$ 6584; [SII] $\lambda\lambda$ 6717,31; [OII] $\lambda$ 7320; [SIII] $\lambda$ 9531) allow us to compute electron densities, temperatures, and ionic abundances. We find internal variations and gradients in electron density. However, the electron temperature and the total oxygen abundance are quite homogeneous. Comparing the mean resolved oxygen abundance with the integrated measurement of the full LVM pointing, we detect no significant under- or overestimations.

## Motivation

The chemical abundance of the interstellar medium (ISM) sets the initial conditions for star formation and provides a probe of chemical galaxy evolution models. Since metals act as coolants in the gas, we can obtain the gas abundances of HII regions by measuring the electron temperature through emission lines. If the electron temperature is not homogeneous across an HII region due to winds, shocks or different ionizing sources, then the abundances of any integrated HII region would be systematically underestimated. With LVM we can measure these variations across a large scale for the first time, since it will observe around 260 such regions inside the Milky Way (Drory et al. 2024), providing a systematic overview of how unresolved nebular structures impact our integrated (extragalactic) prescriptions, especially in more complex star-forming structures. Our first object of choice, the Trifid Nebula, is a HII region ionized by the single O7.5 V star HD 164492A, making it the ideal laboratory for probing spherical symmetries and inhomogeneities inside a single Strömgren sphere.

## LVM data

We combine 8 early LVM science frames (taken during September 27 to 30, 2023) that are reduced using version 1.0.3 of LVMs Data Reduction Pipeline (Mejia et al. in prep.), which removes instrumental features, sky emission and calibrates the flux. We fit the emission lines and the continuum simultaneously using Gaussian profiles for the former and a linear profile for the latter. We correct the fluxes for reddening using various Balmer/Paschen line ratios. The physical properties (electron density, temperature, ionic abundances) are calculated with the PYNEB package (Luridiana et al. 2015) together with the Machine Learning routine AI4NEB to fasten the process.

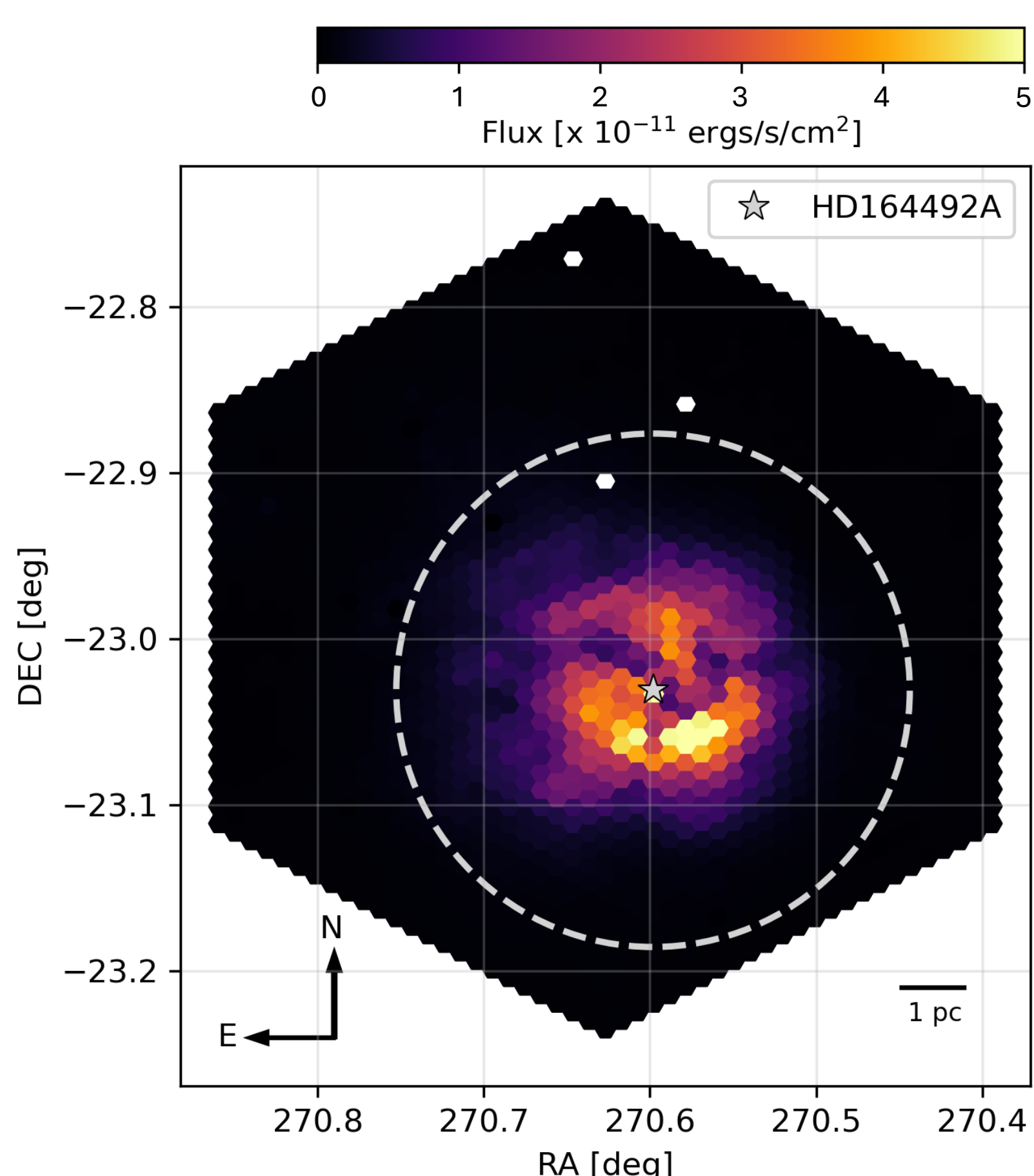


Figure 1: LVM H $\alpha$  flux map of M 20 from Gaussian emission line fits without any corrections. The position of the central ionizing source HD 164492A is marked with a grey star and the theoretical Strömgren sphere of a O7.5 V star (Draine 2011) is indicated by the dashed circle.

## Maps of electron density, temperature & oxygen abundance

The electron densities (Fig. 2) show a negative radial gradient and some discrete regions of enhanced density. This negative radial density gradient was also previously observed in other compact HII regions (Binette et al. 2002; Osterbrock & Ferland 2006; McLeod et al. 2016; Jin et al. 2023). The higher density south-eastern of HD 164492A spatially corresponds with the TC 2 molecular column (Hester et al. 2004; Rho et al. 2008), a large collection of molecular gas that gets hit by ionizing photons, building an ionization front and producing a higher electron density.

The mean values of the resolved electron densities are:  $n_e(\text{[OII]}) = 75 \pm 34 \text{ cm}^{-3}$  and  $n_e(\text{[SII]}) = 100 \pm 37 \text{ cm}^{-3}$ .

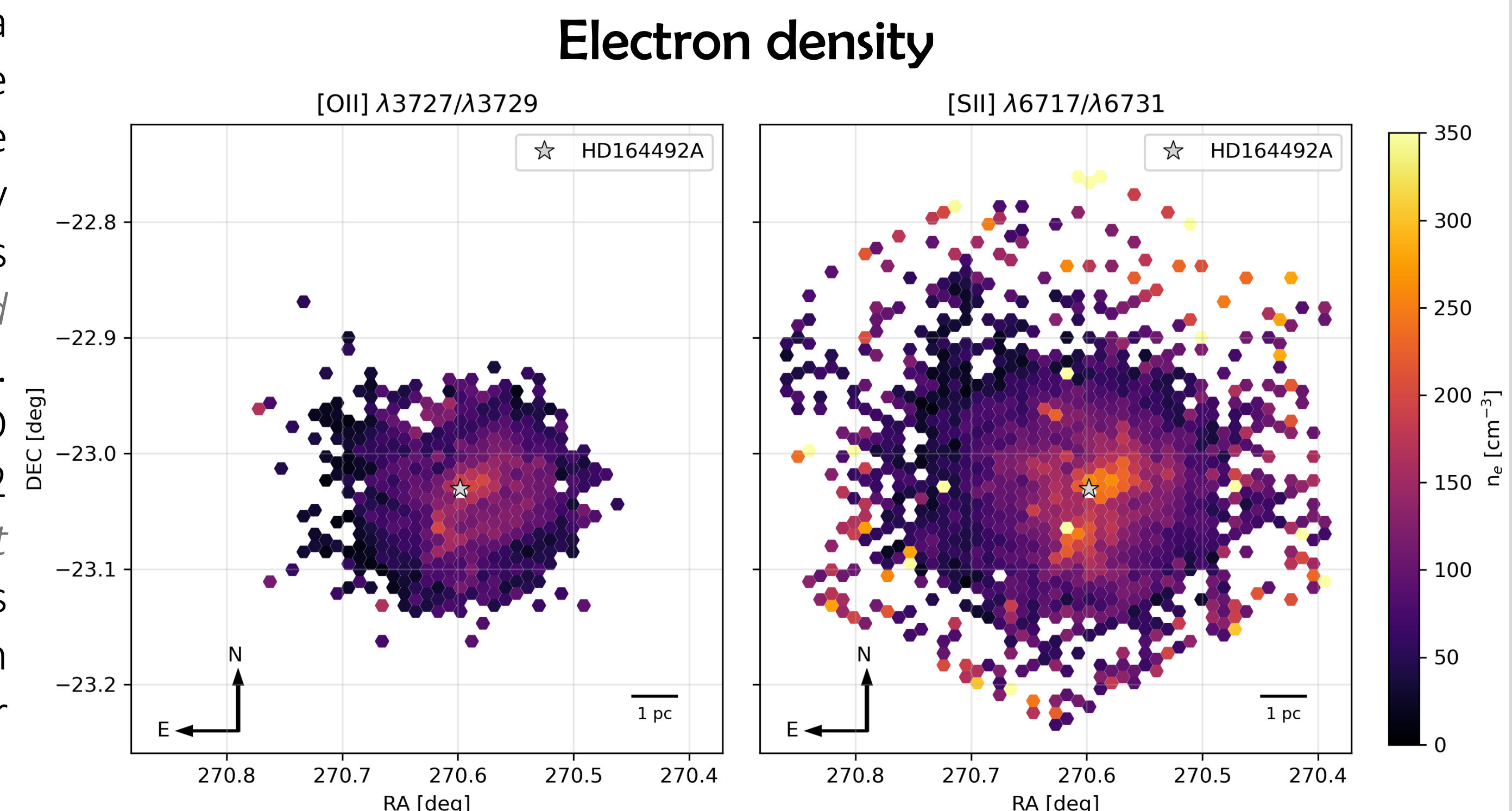


Figure 2: Spatially resolved maps of the electron densities using the [OII] (left) and [SII] (right) doublets. The position of the central ionizing source HD 164492A is marked with a grey star.

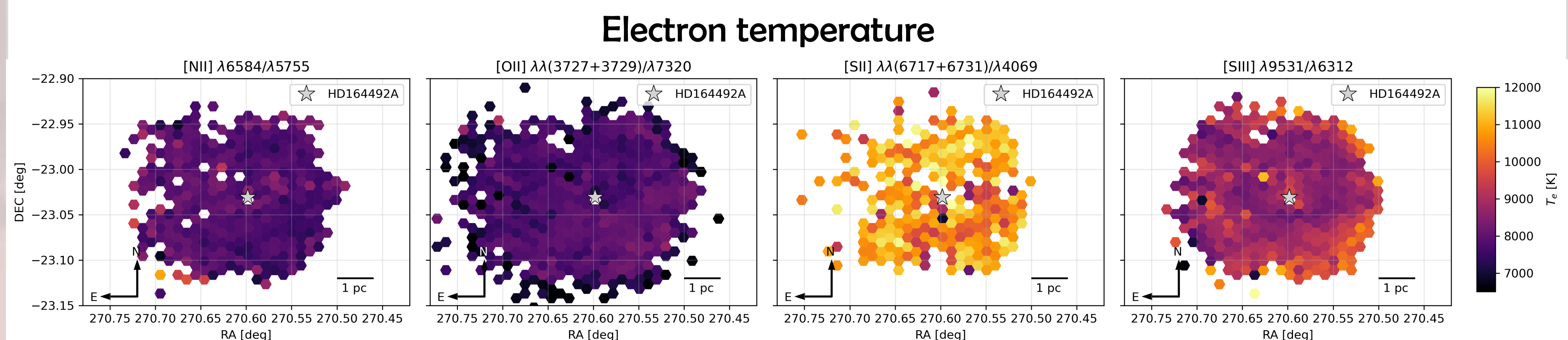


Figure 3: Spatially resolved maps of the electron temperatures using the [NII], [OII], [SII] and [SIII] lines (from left to right). The position of the central ionizing source HD 164492A is marked with a grey star.

The electron temperatures (Fig. 3) are quite homogeneous without any strong gradients. The mean values of the resolved temperatures are:  $T_e(\text{[NII]}) = 7824 \pm 289 \text{ K}$ ,  $T_e(\text{[OII]}) = 7879 \pm 258 \text{ K}$ ,  $T_e(\text{[SII]}) = 10804 \pm 622 \text{ K}$ ,  $T_e(\text{[SIII]}) = 8658 \pm 365 \text{ K}$ .

Our resolved measurement of the absolute oxygen abundance (mean of  $8.61 \pm 0.08 \text{ dex}$ ) is quite homogeneous and in-between the calculations of García-Rojas et al. (2006) that include temperature inhomogeneities of (8.67 dex) and the one that excludes temperature inhomogeneities (8.53 dex). Still, it remains closer to the inhomogeneous assumption.

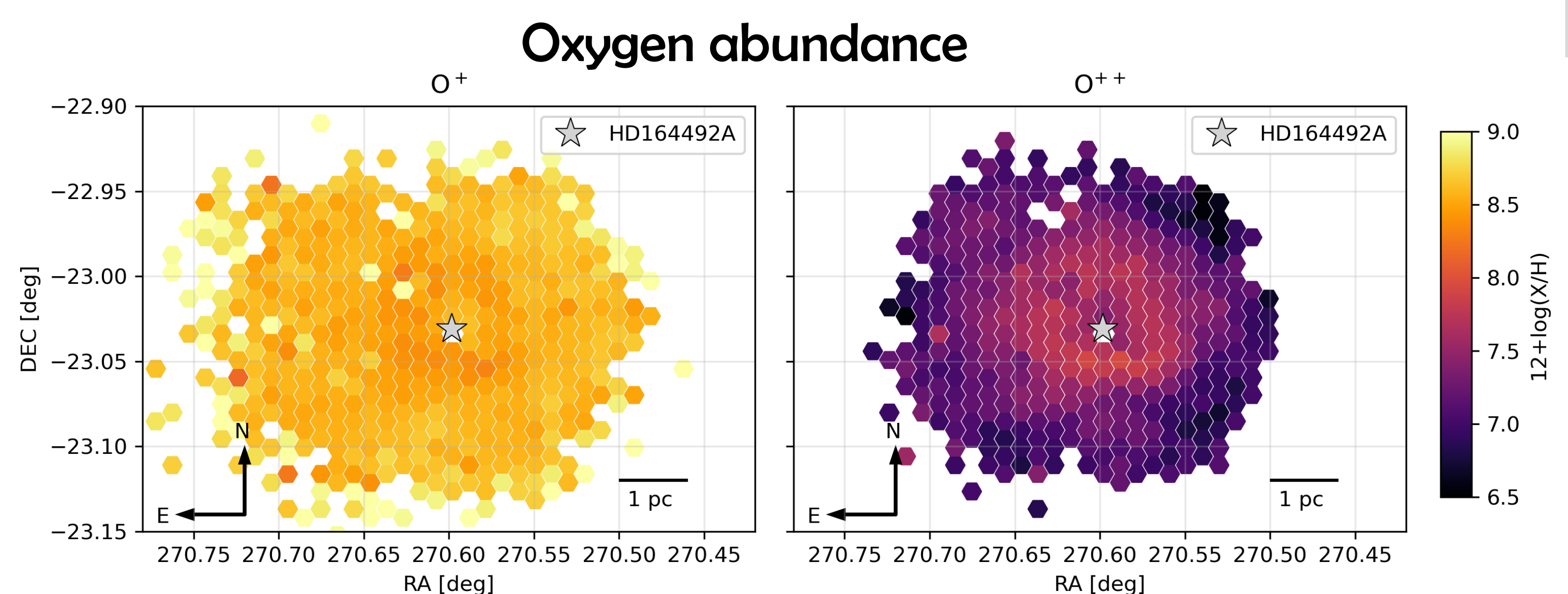


Figure 4: Spatially resolved maps of the O<sup>+</sup> (left) and O<sup>++</sup> (right) abundances. The position of the central ionizing source HD 164492A is marked with a grey star.

Comparing resolved and integrated measurements of the full LVM pointing (see Fig. 1), we detect quite similar electron densities:  $n_e(\text{[OII]}) = 66 \pm 22 \text{ cm}^{-3}$  and  $n_e(\text{[SII]}) = 101 \pm 8 \text{ cm}^{-3}$ . The integrated measurements of the electron temperatures are:  $T_e(\text{[NII]}) = 8007 \pm 697 \text{ K}$ ,  $T_e(\text{[OII]}) = 7372 \pm 138 \text{ K}$ ,  $T_e(\text{[SII]}) = 9142 \pm 1428 \text{ K}$ ,  $T_e(\text{[SIII]}) = 8640 \pm 570 \text{ K}$ . Here,  $T_e(\text{[OII]})$  is underestimated compared to the resolved view. The integrated oxygen abundance  $12+\log(\text{O}/\text{H}) = 8.66 \pm 0.11 \text{ dex}$  includes the inhomogeneous temperature assumption of García-Rojas et al. (2006) and our mean resolved value.

Even if we do not detect significant large scale inhomogeneities in the electron temperatures in our resolved view at 0.24 pc resolution, we cannot rule out inhomogeneities on smaller scales. Also, differences between the resolved and integrated view might be more striking in more complex star-forming regions with e.g. multiple ionizing sources.

## Future work

With a new DRP version, where some current issues with the flux calibration will be fixed, it is planned to include measurements using the absolute fluxes like: H $\beta$  electron density, filling factor, amount of ionizing photons and contribution of the nebula to diffuse ionized gas.

Further, we will repeat this kind of analysis on other star-forming regions (e.g. 30 Doradus).

## References

- Binette L., González-Gómez D. I., Mayya Y. D., 2002, *Rev. Mex. Astron. Astrofis.*, 38, 279
- Draine B. T., 2011, *Physics of the Interstellar and Intergalactic Medium*
- Drory N., Blanc G. A., Kreckel K., et al. 2024, *arXiv e-prints*, arXiv:2405.01637, doi: 10.48550/arXiv.2405.01637
- García-Rojas J., Esteban C., Peimbert M., Costado M. T., Rodríguez M., Peimbert A., Ruiz M. T., 2006, *MNRAS*, 368, 253
- Hester J. J., Desch S. J., Healy K. R., Leshin L. A., 2004, *Science*, 304, 1116
- Jin Y., Sutherland R., Kewley L. J., Nicholls D. C., 2023, *ApJ*, 958, 179
- Luridiana V., Morisset C., Shaw R. A., 2015, *A&A*, 573, A42
- McLeod A. F., et al., 2016, *MNRAS*, 462, 3537
- Osterbrock D. E., Ferland G. J., 2006, *Astrophysics of gaseous nebulae and active galactic nuclei*
- Rho J., Lefloch B., Reach W. T., Cernicharo J., 2008, in *Reipurth B., ed., Vol. 5, Handbook of Star Forming Regions, Volume II*, p. 509
- <https://github.com/Morisset/AI4NEB>

## Download



scan me